J|A|C|S
ARTICLES
Published on Web 12/15/2006

Unusual Crystallization Behaviors of Anatase Nanocrystallites from a Molecularly Thin Titania Nanosheet and Its Stacked Forms: Increase in Nucleation Temperature and Oriented Growth

Katsutoshi Fukuda,[†] Yasuo Ebina,[†] Tatsuo Shibata,[†] Takashi Aizawa,[†] Izumi Nakai,[‡] and Takayoshi Sasaki*,[†]

Contribution from the Nanoscale Materials Center, National Institute for Materials Science, 1-1 Namiki, Tsukuba, Ibaraki 305-0044, Japan, and Department of Applied Chemistry, Tokyo University of Science, 1-3 Kagurazaka, Shinjuku, Tokyo 162-8601, Japan

Received September 21, 2006; E-mail: sasaki.takayoshi@nims.go.jp

Abstract: Crystallization behaviors of anatase nanocrystallites from an ultrathin two-dimensional reactant composed of exfoliated titania nanosheets have been studied by monitoring the heating process of their well-organized films, with which the film thickness can be controlled from a molecularly thin monolayer to a stacked multilayer structure with a stepwise increment of ~1 nm. The heated products were identified by means of total reflection fluorescence X-ray absorption near-edge structure analysis and in-plane X-ray diffraction measurements using a synchrotron radiation source. The films composed of five or more layers of stacked nanosheets were transformed into anatase at 400−500 °C, which is a normal crystallization temperature of anatase from bulk reactants. As the film became thinner by decreasing the number of nanosheet layers to five or less, the crystallization temperature was found to increase and finally reached 800 °C for the monolayer film. Interestingly, preferential growth of anatase along the *c*-axis was strongly promoted for these ultrathin films. These unusual behaviors may be understood in terms of crystallization from the two-dimensional system of scarcely distributed reactants. The titania nanosheet crystallite is much thinner than the unit cell dimensions of anatase, and therefore, extensive atomic diffusion is required for the transformation particularly for the ultrathin films with a critical number (2−3) of stacked nanosheet layers. There is some structural similarity between anatase and titania nanosheet, which may account for the oriented growth of anatase nanocrystallites.

Introduction

Control of crystallization behavior has become a matter of concern in physical and material science. Fundamental theories regarding the nucleation and growth dynamics of crystalline materials from various systems such as gas, liquid, and solid phases have been advocated,[1,2] contributing to the development of advanced functional materials in the past decade. In particular, with the rapid progress in material design in the nanometer-scale regime, the fine control of crystal growth has developed. Several groups have reported the crystallization of inorganic materials such as calcium carbonate on a micropatterned surface of self-assembled films,[3] which offers compartmented areas of different nucleation activity. This approach makes it possible to control the size, population, and crystallographic orientation of grown crystals as well as their lateral positioning. On the other hand, Johnson and collaborators carried out elaborate studies on crystallization of inorganic materials by annealing superlattice multilayers designed by beam epitaxy technology.[4] The artificial multilayers as a three-dimensional reactant allow atomic diffusion and nucleation activities to be freely modified, and this strategy yielded some metastable crystalline phases that are unable to be trapped under ordinary conditions.

These recent studies by utilizing so-called nanochemistry have yielded tremendously attractive findings and opened a new research field. However, there are other unexplored nanosystems that may lead to some novel phenomena. For example, knowledge on crystallization from a two-dimensional solid system with a thickness of nanometer-scale range is still very limited. The effect of its thickness, namely the abundance of

[†] National Institute for Materials Science.
[‡] Tokyo University of Science.

(1) (a) Zeng, X. C.; Oxtoby, D. W. *J. Chem. Phys.* **1991**, *94*, 4472−4478. (b) Viisanen, Y.; Strey, R.; Reiss, H. *J. Chem. Phys.* **1993**, *99*, 4680−4692. (c) Weakliem, C. L.; Reiss, H. *J. Chem. Phys.* **1994**, *101*, 2398−2406. (d) McGraw, R.; Laaksonen, A. *Phys. Rev. Lett.* **1996**, *76*, 2754−2757. (e) Liu, X. Y.; Maiwa, K.; Tsukamoto, K. *J. Chem. Phys.* **1997**, *106*, 1870−1879. (f) Bowles, R. K.; McGraw, R.; Schaaf, P.; Senger, B.; Voegel, J.-C.; Reiss, H. *J. Chem. Phys.* **2000**, *113*, 4524−4532.
(2) (a) Zhang, H.-Z.; Banfield, J. F. *J. Mater. Chem.* **1998**, *8*, 2073−2076. (b) Zhang, H.-Z.; Banfield, J. F. *Chem. Mater.* **2002**, *14*, 4145−4154.
(3) Aizenberg, J.; Black, A. J.; Whitesides, G. M. *Nature* **1999**, *398*, 495−498.
(4) (a) Noh, M.; Johnson, D. C. *J. Am. Chem. Soc.* **1996**, *118*, 9117−9122. (b) Williams, J. R.; Johnson, M.; Johnson, D. C. *J. Am. Chem. Soc.* **2001**, *123*, 1645−1649. (c) Williams, J. R.; Johnson, D. C. *Inorg. Chem.* **2002**, *41*, 4127−4130. (d) Jensen, J. M.; Ly, S.; Johnson, D. C. *Chem. Mater.* **2003**, *15*, 4200−4204.

 10.1021/ja0668116 CCC: $37.00

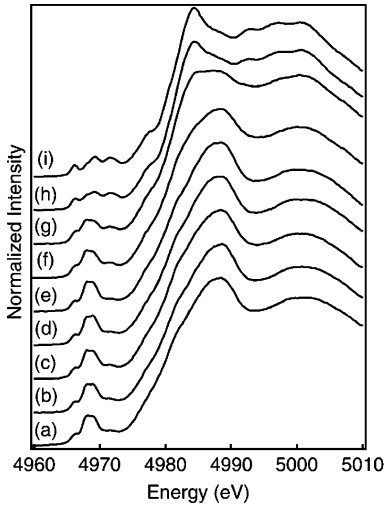

Figure 1. XANES spectra for (a) as-grown monolayer film and that heated at (b) 300, (c) 400, (d) 500, (e) 600, (f) 700, (g) 800, (h) 900 °C, and (i) reference (anatase).

reactant, on the crystallization behavior would be of particular interest. Nucleation and crystal growth may be severely hindered in such a two-dimensionally bound reactant.

Recently, a wide variety of layered host materials, ranging from clay minerals[5] to transition metal oxides,[6−8] chalcogenides,[9] and so on, have been delaminated into colloidal elementary layers through soft-chemical processes. The resulting unilamellar crystallites have been named nanosheets because of their peculiar structural features with extremely high two-dimensional anisotropy. Their thickness is in the range of molecular dimensions, mostly around 1 nm, while the lateral dimension is usually in the micrometer range, roughly corresponding to a size of precursor layered crystals. These colloidal nanosheets can be deposited via alternate adsorption with some oppositely charged polyelectrolytes to produce multilayer ultrathin films with a controlled nanoarchitecture.[10] We have demonstrated that sequential adsorption of titania nanosheets of $Ti_{1-\delta}O_2$ ($\delta \approx 0.09$) and poly(diallyldimethylammonium) (PDDA) cations can grow multilayer films at an increment step of 1−2 nm, which corresponds to the thickness of the bilayer, PDDA/$Ti_{1-\delta}O_2$.[10c] These films should be employed as a model reactant in the investigation mentioned above for the control of crystallization. In fact, we have found intriguing phenomena in the crystallization process of anatase from a "monolayer" film

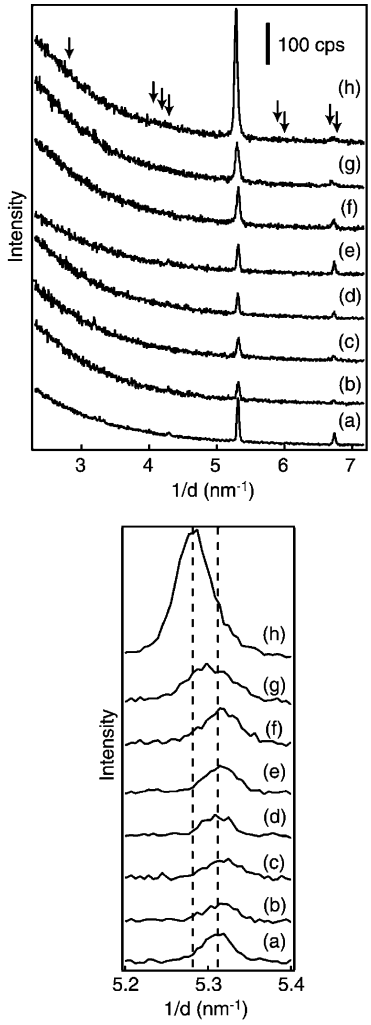

Figure 2. In-plane XRD patterns for (a) as-grown monolayer film and that heated at (b) 300, (c) 400, (d) 500, (e) 600, (f) 700, (g) 800, and (h) 900 °C. Lower panel shows the magnified profile around 5.3 nm^{-1}.

of titania nanosheets.[11] The nanosheet structure was stable up to a temperature of 800 °C, which is much higher than the normal crystallization temperature of anatase. Although the results were very enticing, it is difficult to pursue this phenomenon in depth to obtain a clear understanding of it because the films were not necessarily of satisfactory quality for the purpose. The deposition of the nanosheets onto the oppositely charged surface inevitably results in some overlap of the nanosheets as well as gaps between them. In practice, the "monolayer" film used in the previous study was far from the ideal monolayer, showing overlapped regions of 45% in a total covered area of 90%.[12] This severe overlap makes it difficult to precisely interpret the crystallization behavior because the "monolayer" film practically includes a significant proportion of the "bilayer" region. It is obviously impossible to explore how the film thickness affects the crystallization behavior because the multilayer films should have a more disorganized architecture.

High-quality films without extensive overlapped patches and uncovered areas are essential for such studies. Most recently,

(5) (a) Walter, G. F. *Nature* **1960**, *187*, 312−313. (b) Nadeau, P. H.; Wilson, M. J.; McHardy, W. J.; Tait, J. M. *Science* **1984**, *225*, 923−925.
(6) (a) Treacy, M. M. J.; Rice, S. B.; Jacobson, A. J.; Lewandowski, J. T. *Chem. Mater.* **1990**, *2*, 279−286. (b) Schaak, R. E.; Mallouk, T. E. *Chem. Mater.* **2002**, *14*, 1455−1471. (c) Takagaki, A.; Lu, D.; Kondo, J. N.; Hara, M.; Hayashi, S.; Domen, K. *Chem. Mater.* **2005**, *17*, 2487−2489. (d) Miyamoto, N.; Yamamoto, H.; Kaito, R.; Kuroda, K. *Chem. Commun.* **2002**, 2378−2379.
(7) (a) Sasaki, T.; Watanabe, M.; Hashizume, H.; Yamada, H.; Nakazawa, H. *J. Am. Chem. Soc.* **1996**, *118*, 8329−8335. (b) Sasaki, T.; Watanabe, M. *J. Am. Chem. Soc.* **1998**, *120*, 4682−4689. (c) Sugimoto, W.; Terabayashi, O.; Murakami, Y.; Takasu, Y. *J. Mater. Chem.* **2002**, *12*, 3814−3818. (d) Miyamoto, N.; Kuroda, K.; Ogawa, M. *J. Mater. Chem.* **2004**, *14*, 165−170.
(8) (a) Liu, Z.-H.; Ooi, K.; Kanoh, H.; Tang, W.-P.; Tomida, T. *Langmuir* **2000**, *16*, 4154−4164. (b) Omomo, Y.; Sasaki, T.; Wang, L. Z.; Watanabe, M. *J. Am. Chem. Soc.* **2003**, *125*, 3568−3575.
(9) (a) Leaf, A.; Schöllhorn, R. *Inorg. Chem.* **1977**, *16*, 2950−2956. (b) Joensen, P.; Frindt, R. F.; Morrison, S. R. *Mater. Res. Bull.* **1986**, *21*, 457−461. (c) Yang, D.; Frindt, R. F. *J. Phys. Chem. Solids* **1996**, *57*, 1113−1116.
(10) (a) Kleinfeld, E. R.; Ferguson, G. S. *Science* **1994**, *265*, 370−373. (b) Kaschak, D. M.; Lean, J. T.; Waraksa, C. C.; Saupe, G. B.; Usami, H.; Mallouk, T. E. *J. Am. Chem. Soc.* **1999**, *121*, 3435−3445. (c) Sasaki, T.; Ebina, Y.; Watanabe, M.; Decher, G. *Chem. Commun.* **2000**, 2163−2164.
(11) Fukuda, K.; Sasaki, T.; Watanabe, M.; Nakai, I.; Inaba, K.; Omote, K. *Cryst. Growth Des.* **2003**, *3*, 281−283.
(12) Sasaki, T.; Ebina, Y.; Tanaka, T.; Harada, M.; Watanabe, M.; Decher, G. *Chem. Mater.* **2001**, *13*, 4661−4667.

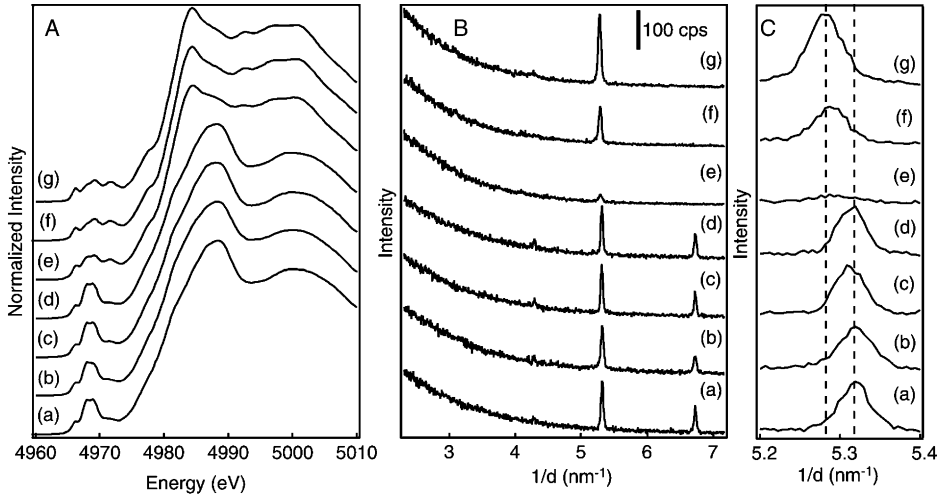

Figure 3. (A) XANES spectra and (B) in-plane XRD patterns for the two-layer films heated at (a) 300, (b) 400, (c) 500, (d) 600, (e) 700, (f) 800, and (g) 900 °C. (C) Magnified profile around 5.3 nm^{-1}.

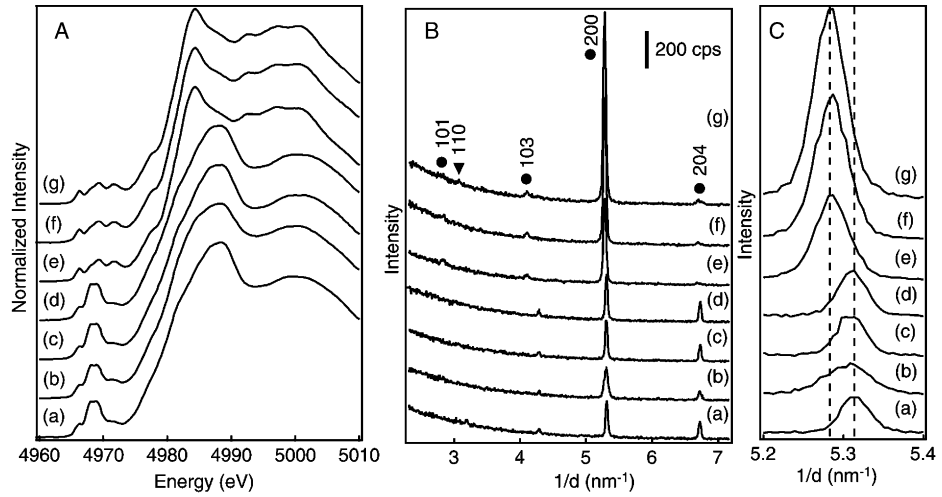

Figure 4. (A) XANES spectra and (B) in-plane XRD patterns for the three-layer films heated at (a) 300, (b) 400, (c) 500, (d) 600, (e) 700, (f) 800, and (g) 900 °C. (●) and (▼) show the indices of anatase and rutile, respectively. (C) Magnified profile around 5.3 nm^{-1}.

we developed a new procedure to fabricate highly organized films of nanosheets suitable for the study.[13,14] The sequential adsorption of oversized titania nanosheets (~30 μm in lateral size) followed by ultrasonic treatment could produce a nearly perfect film through trimming of overlapped nanosheets. Under optimized conditions, overlap and gap were suppressed to 6% and a negligible level, respectively, and deposition with this quality could be repeated to produce well-ordered multilayer structures. With these neat films, the thickness can be accurately controlled by varying the number of deposition cycles.

Here, we report interesting crystallization behaviors in the heating process of the monolayer and multilayer films thus obtained. The crystallization temperature of anatase was dependent on the thickness, and bulk behavior appeared for the films thicker than ~5 nm. Furthermore, preferential oriented growth of anatase nanocrystallites with respect to the precursor nanosheets was observed, suggesting some templating effect of the nanosheet.

Experimental Section

Material Synthesis. Single crystals of starting layered titanate, $K_{0.8}Ti_{1.73}Li_{0.27}O_4$, were synthesized by slow-cooling a K_2MoO_4 flux melt containing a stoichiometric mixture of K_2CO_3, Li_2CO_3, and TiO_2 from 1473 to 1223 K.[15] The obtained crystals were treated with a 0.5 mol dm^{-3} HCl solution for 3 days to be converted into an acid-exchanged form, $H_{1.07}Ti_{1.73}O_4 \cdot H_2O$.[15] The protonic titanate crystals (0.4 g) were immersed in 100 cm^3 of a 0.025 mol dm^{-3} tetrabutylammonium hydroxide (TBAOH) solution with intermittent gentle shaking for two weeks. The resulting colloidal suspension contained unilamellar titania nanosheets of composition $Ti_{0.87}O_2$ with an average lateral size of 30 μm.

These large-sized titania nanosheets were deposited onto a substrate into highly organized monolayer and multilayer films by our recently developed method, which involved electrostatic self-assembly and subsequent ultrasonic treatment.[13] Substrates of Si wafers and quartz glasses were immersed in a bath of 1/1 CH_3OH/HCl and *conc*H_2SO_4 for 30 min each for cleaning. The substrates were precoated by being dipped in a PDDA chloride solution (pH = 9, 20 g dm^{-3}). Titania nanosheets were adsorbed onto the primed substrate by immersing it

(13) Tanaka, T.; Fukuda, K.; Ebina, Y.; Takada, K.; Sasaki, T. *Adv. Mater.* **2004**, *16*, 872−875.
(14) Osada, M.; Ebina, Y.; Funakubo, H.; Yokoyama, S.; Kiguchi, T.; Takada, K.; Sasaki, T. *Adv. Mater.* **2006**, *18*, 1023−1027.
(15) Tanaka, T.; Ebina, Y.; Takada, K.; Kurashima, K.; Sasaki, T. *Chem. Mater.* **2003**, *15*, 3564−3568.

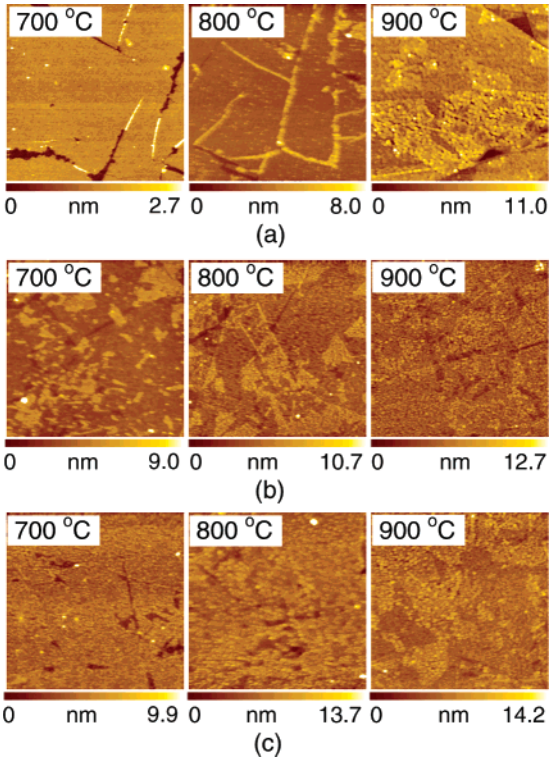

Figure 5. AFM images ($3 \times 3\ \mu m^2$) for (a) monolayer, (b) two-layer, and (c) three-layer films heated at 700, 800, and 900 °C.

in the nanosheet suspension (pH = 9, 0.08 g dm^{-3}) for 20 min. The film was washed carefully with ultrapure water and then subjected to an ultrasonic field in the TBAOH solution (pH = 11). This treatment removes the overlapped region of nanosheets, as reported previously, leading to a highly organized monolayer film with negligible gaps and overlaps between the nanosheets.[13] Repetition of these operations yielded multilayer films composed of a specified number of layer pairs of the titania nanosheet and PDDA. Heat treatments of these films were performed by increasing the temperature from ambient temperature at a rate of 5 °C min^{-1} to a preset temperature (300, 400, 500, 600, 700, 800, and 900 °C). After keeping the samples at that temperature for 1 h, we cooled them naturally in a furnace.

Measurements and Analysis. X-ray absorption near-edge structure measurements were carried out in total reflection fluorescence mode (TRF-XANES) at the Photon Factory BL-12C in the Institute of Materials Structure Science, High Energy Accelerator Research Organization (KEK-PF). Synchrotron radiation X-ray monochromated by Si(111) double crystals was slit to produce a square beam of 0.2×2 mm^2. The incident angle to the sample surface was fixed below the critical angle (~0.5°) for the total external reflection decided from the premeasurement of the X-ray reflectivity curve. Ti K-edge XANES spectra were recorded in an energy range from 4960 to 5010 eV with an interval of 0.3 eV. The fluorescence X-ray intensity was detected by a 19-element Ge solid-state detector arranged in the horizontal plane of the substrate, while the incident X-ray intensity was monitored by an ionization chamber. XANES spectra were calculated from the intensity ratio of the fluorescence X-ray to the incident X-ray.

In-plane X-ray diffraction (XRD) analysis was performed with a four-axis diffractometer installed at the BL-3A in KEK-PF. The incident X-ray was monochromated and focused on the incident slit (0.1 mm) by Si(111) sagittal focusing double monochromators and two Pt mirrors fused on quartz. The resultant horizontal and vertical divergences were 0.15° and 0.30°, respectively. The incident angle to the sample surface was fixed below the critical angle of total external reflection. The diffracted X-ray that passed through the soller slit (0.45°) at the front side of the NaI scintillation counter was counted for 3 s at each sampling point (angular interval of 0.05°).

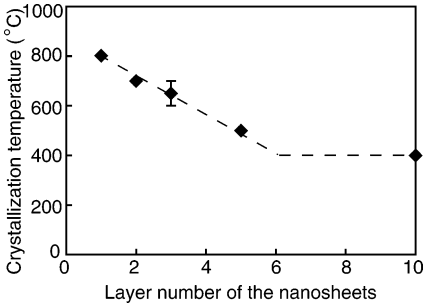

Figure 6. Layer number dependence of the temperature for transformation into anatase.

A tapping-mode atomic force microscope (Seiko Instruments SPA400 AFM system) with a Si tip cantilever (40 N m^{-1}) was used to examine the topographical change during the heat treatment.

Results and Discussion

Starting Films of the Nanosheets. The deposition of the large-sized nanosheets followed by the ultrasonic treatment produced a high-quality monolayer film (Supporting Information, Figure S1), consistent with our previous report. The film was composed of densely packed nanosheets with negligible gaps between them. Neighboring sheets were slightly overlapped with each other, and the boundaries were perceived as narrow strings (~1 nm higher than the other region), yielding a weblike pattern. The height analysis of its AFM image revealed a total surface coverage of nearly 100% with overlapping area of 6%. This highly organized packing of the nanosheets was greatly improved compared with similar films of small-sized nanosheets (average lateral size: 500 nm) derived from a polycrystalline sample of the layered titanate. In the latter films, the overlap patches are usually 45% when the total coverage is ~90%.[12]

Repetition of the deposition procedure involving the ultrasonification yielded a multilayer film, which was confirmed by progressive enhancement of UV absorption due to the nanosheet. The AFM image suggested that the highly organized film texture was maintained, although it became more difficult to resolve the nanosheets for the larger number of deposition cycles due to a gradual increase in surface roughness. The films showed a sharp Bragg XRD peak attributable to the well-ordered multilayer structure, which is similar to our previous results.[13] This diffraction feature again supports the formation of high-quality multilayer films, which should be suitable for the present study. On the other hand, the random in-plane orientation of the nanosheets was confirmed by RHEED measurement at various azimuth angles. Thus, the system can be described as a fiber crystal.

Thermally Induced Structural Transformation of the Monolayer Film. Figure 1 shows Ti K-edge XANES spectra in the heating process up to 900 °C for the monolayer film of titania nanosheets. The spectrum of the as-prepared film is attributable to the titania nanosheets. The spectral profile is different from that of reference anatase in terms of intensity distribution of pre-edge feature (4964−4974 eV) and the location of white line peaks (4980−4995 eV), which reflect a structural local symmetry. Thus, these differences can be employed as an indicator to follow the transformation from the nanosheet to anatase. There was no signature of anatase up to

700 °C. The features diagnostic of anatase (e.g., a sharp peak at 4984.4 eV and the pre-edge feature) appeared and overlapped with the characteristic pattern of the nanosheet in the sample heated at 800 °C. Their abundance was estimated to be ~85% for the nanosheet and ~15% for anatase by decomposition of the spectrum. Heating at a higher temperature of 900 °C completed the transformation into a single phase of anatase.

The in-plane XRD measurements provided another clue to monitor this structural change from a different viewpoint (Figure 2). The as-grown film prepared on the Si wafer exhibited three sharp diffraction peaks at 4.28, 5.31, and 6.73 nm^{-1}, which are indexable to 11, 20, and 02, respectively, for a face-centered rectangular unit cell (0.3760(1) nm × 0.2967(2) nm) of the titania nanosheet.[16,17] At first glance, there appeared to be a negligible change in pattern except for an intensity decay of the 11 and 02 peaks. However, the expanded pattern showed a distinct change in the position of the most prominent peak that appeared around 5.3 nm^{-1}. There was a negligible change up to 700 °C, but a clear shift of the peak was observed above 800 °C. The resultant peak position at 900 °C exactly coincides with that of the 200 reflection for anatase (5.28 nm^{-1}), which is consistent with the XANES data. The diffraction feature at 800 °C may be interpreted as an intermediate profile between the two phases. This structural change is not a genuine phase transformation, but may be formulated in terms of the following process involving the release of some water molecules:

$$0.52H^{+}/Ti_{0.87}O_2^{0.52-}(\text{nanosheet}) \rightarrow 0.87TiO_2(\text{anatase}) + 0.26H_2O(g) \quad (1)$$

The protons on the left side of the above equation or ammonium ions should be present or formed in the heating process as a decomposition fragment of organic substances.[18]

Importantly, only the 200 reflection was observed in the in-plane data for the sample after the transformation to anatase, although polycrystalline anatase should exhibit many reflections in this range as indicated by the arrows. Preferential growth of anatase crystallites along its *c*-axis may account for this diffraction feature. RHEED data (Supporting Information, Figure S2) further supported this unique crystallographic orientation, showing rows of diffraction spots extending along the *c**-axis.

These structural changes from the nanosheet monolayer into anatase oriented along the *c*-axis above 800 °C basically agree with our previous results using the film of smaller-sized nanosheets.[11] The final product at 900 °C from the film of small-sized nanosheets contained a small amount of rutile and non-oriented anatase phase, which was not the case for the film in the present study. This may be a consequence of the mean film quality with a substantial amount of overlapped area. A thicker region in the films or the overlapped patches of the nanosheets tends to yield non-oriented crystallites, as will be described below.

Thermal Behavior of the Multilayer Films. XANES data and in-plane XRD profiles for two- and three-layer films of the nanosheets are displayed in Figures 3 and 4, respectively. The nanosheet structure remained unchanged up to 600 °C for the two-layer film, while the structural transformation above 700 °C was indicated consistently by XANES and in-plane XRD data. The diffraction peak for the sample heated at 700 °C was weak and enhanced again upon heating at higher temperatures. This may indicate that the transformation took place exactly at this temperature. It is known that the structural change often involves some disorder.

The three-layer film underwent a similar structural change at a slightly lower temperature (between 600 and 700 °C), as can be derived from the data in Figure 4. One of the noticeable features is that some weak peaks assignable to anatase, indicated by circles, were detected in addition to the strong 200 reflection. This suggests that polycrystalline crystallites started to form although the preferential orientation was still predominant. Note that the 101 reflection is the strongest and approximately double that of the 200 peak in intensity for polycrystalline anatase.[19]

The crystallization temperature continued to decrease for the thicker films. XANES patterns and in-plane XRD profiles for five- and 10-layer films of the nanosheets indicate that these samples transformed into anatase at 400−500 °C and 400 °C, respectively (Supporting Information, Figures S3 and S4). These temperatures are close to that of bulk titania-based materials, which usually crystallize as polycrystalline anatase at 400−500 °C.[20,21] Furthermore, the abundance of non-oriented anatase tended to increase for these thicker films, while the 200 peak was the strongest, suggesting that the orientation was still significant.

Figure 5 shows the topographical features for the samples in the temperature range where the transformation took place. Note that the AFM images of the five- and 10-layer samples were not resolved well enough to identify individual crystallites, which was probably due to a large surface roughness. There was no noticeable change in texture for the monolayer film heated at 700 °C. The initiation of anatase crystallization at 800 °C is clearly detected by the formation of granular crystallites showing a height of ~3 nm larger than the nanosheet. The abundance of anatase may be consistent with that of 15% deduced from the XANES analysis. Interestingly, the crystallized anatase formed a line pattern, which suggests that the crumple or edge of the nanosheets provides a more active site for the transformation. The monolayer nanosheets changed completely at 900 °C into granular particles with a lateral size of about 50−100 nm and an average height of 3 nm, which is consistent with the formation of anatase revealed by XANES and in-plane XRD analyses.

The two-layer sample heated at 700 °C was identified as a mixture of the unilamellar sheets and anatase nanocrystals, and the film heated at 800 °C and above was totally composed of nanoparticles. This mixing state at 700 °C gives a reasonable picture of ongoing crystallization, yielding the poorly resolved in-plane diffraction peak. In contrast, the three-layer films showed a well-developed granular texture at 700 °C, confirming the lower transformation temperature in comparison with that of the two-layer film. The average height as well as packing density of anatase nanocrystals tended to increase gradually with

(16) Similar data were obtained for samples on a quartz glass substrate, indicating that the substrates did not affect these structural changes.
(17) Fukuda, K.; Nakai, I.; Ebina, Y.; Tanaka, M.; Mori, T.; Sasaki, T. *J. Phys. Chem. B* **2006**, *110*, 17070−17075.
(18) Sasaki, T.; Ebina, Y.; Fukuda, K.; Tanaka, T.; Harada, M.; Watanabe, M. *Chem. Mater.* **2002**, *14*, 3524−3530.
(19) The Joint Committee for Powder Diffraction Studies, 00-021-1272.
(20) Wang, C.-C.; Ying, J. Y. *Chem. Mater.* **1999**, *11*, 3113−3120.
(21) Sasaki, T.; Watanabe, M.; Michiue, Y.; Komatsu, Y.; Izumi, F.; Takenouchi, S. *Chem. Mater.* **1995**, *7*, 1001−1007.

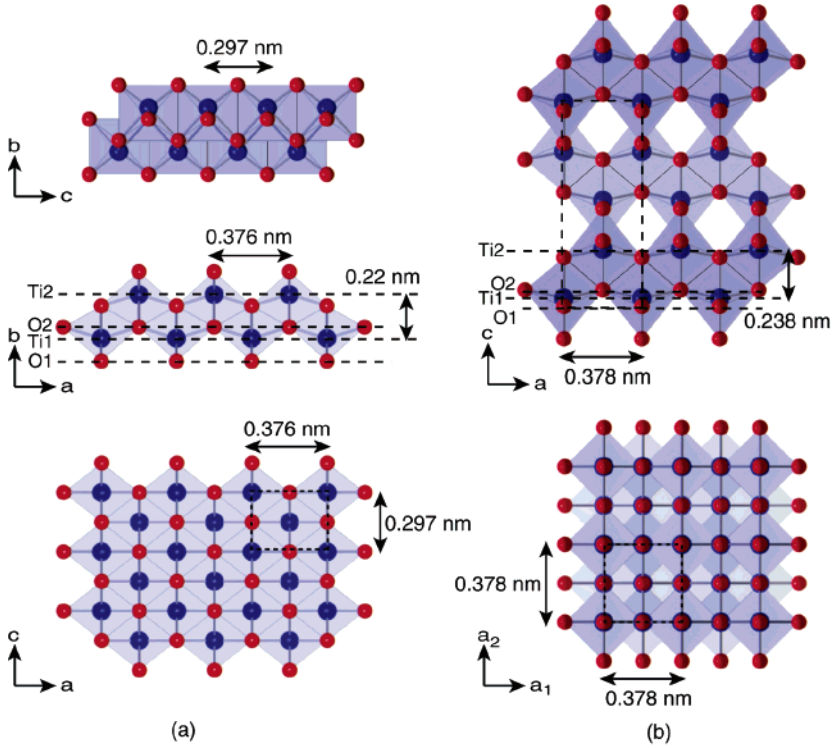

Figure 7. Atomic architecture of (a) titania nanosheet and (b) anatase. Blue and red circles represent Ti and O atoms, respectively. The axis notation of the nanosheet refers to the symmetry of the original layered titanate.

the layer number of nanosheets. On the other hand, their lateral dimensions were nearly unchanged.

The anatase crystallization temperature deduced from the data above is plotted against the layer number in Figure 6. The nanosheet films with the layer number of >5 transformed into anatase at 400−500 °C, which is normal for bulk titania materials. The crystallization temperature increased with the decrease of layer number and attained 800 °C or higher for the monolayer film. This thermal behavior should be closely associated with the abundance of the reactant and its configuration. The five- and 10-layer films can be considered as a reactant system having a substantially adequate amount of three-dimensionally distributed Ti and O atoms. This saturated environment with excessive atoms should allow facile nucleation and rapid growth of thermodynamically stable crystallites of anatase at relatively low temperatures. In contrast, the monolayer film of titania nanosheets consists of two atomic planes of Ti and four atomic planes of O along the film normal as illustrated in Figure 7a.[22] This two-dimensional structure is even thinner than the unit cell dimension of anatase along the *c*-axis, in which four atomic planes of Ti and eight atomic planes of O are included (Figure 7b).[23] The shortage of component atoms to construct the anatase structure may be principally responsible for the inhibition of crystallization at the normal temperature. Both nucleation and growth of anatase from the monolayer state of nanosheets should require extensive thermal activation of atomic diffusion. As revealed by AFM images, the monolayer film of the nanosheets with a thickness of 1 nm was transformed into anatase nanocrystals with a height of about 3 nm, which approximately corresponds to three unit cells of anatase along the *c*-axis. This transformation should be involved by the extensive atomic migration. This situation should be gradually relaxed as the film becomes thicker. For example, the two- and three-layer films have a sufficient distribution of titanium and oxygen atoms to produce the one unit cell of anatase. However, atomic diffusion is still essential for the formation of a critical nucleus. This intermediate atomic diffusion may make the transformation temperatures moderately higher than usual. To summarize, the number of atomic layers in the starting films is a dominant factor for the crystallization temperature provided the film is thinner or comparable to the unit cell dimensions of anatase.

It is important to assess the dependence of the crystallization behavior on the heating time, because the duration of 1 h might be too short to attain the crystallization of anatase. Figure 8 depicts in-plane diffraction patterns of the monolayer sample heated at 600, 700, and 800 °C for 24 h, respectively. These patterns are nearly the same as those of each sample heated for 1 h in terms of shape and peak position, indicating that the nanosheet retains its crystallinity even after heating for a long time. The structure transformation is generally governed by thermodynamics, and the results discussed here may be interpreted as kinetic effects.

Let us consider why the preferential growth of anatase crystals takes place in the present system. As illustrated in Figure 7, an atomic plane of Ti layer, Ti1, sandwiched between the adjacent layers of O atoms, O1 and O2, in the nanosheet is similar to that of anatase. The projections onto the *b*-axis for the nanosheet and onto the *c*-axis for anatase show close similarities in terms of atomic arrangement (Figure 9), except for the following differences: (i) the rectangular unit cell (0.38 nm × 0.30 nm) for the former while the square lattice (0.38 nm × 0.38 nm) for the latter, (ii) vertical displacements of O atoms from the

(22) Fukuda, K.; Nakai, I.; Oishi, C.; Nomura, M.; Harada, M.; Ebina, Y.; Sasaki, T. *J. Phys. Chem. B* **2004**, *108*, 13088−13092.
(23) Burdett, J. K.; Hughbanks, T.; Miller, G. J.; Richardson, J. W.; Smith, J. V. *J. Am. Chem. Soc.* **1987**, *109*, 3639−3646.

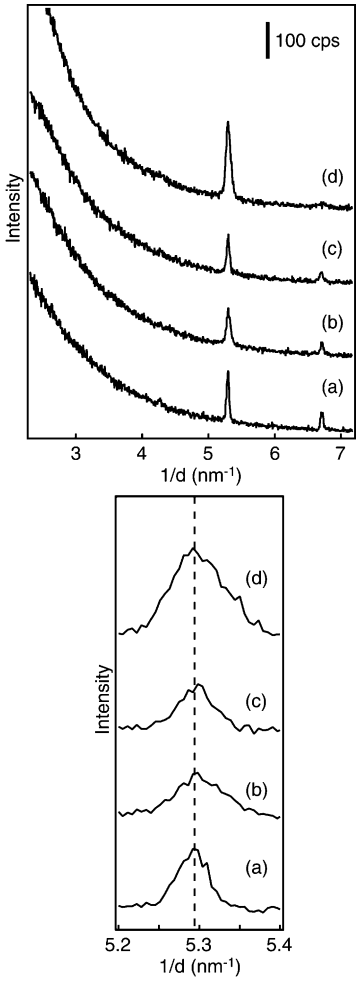

Figure 8. In-plane XRD patterns for (a) as-grown film as a reference sample and heated monolayer films at (b) 600, (c) 700, and (d) 800 °C for 24 h. Lower panel shows the magnified profile around 5.3 nm^{-1}.

Ti atom plane, and (iii) about 13% vacancy at Ti octahedral sites in the former while full occupancy of Ti sites in the latter. This similarity suggests that the set of planes of Ti1, O1, and O2 in the nanosheet acts as an embryo of anatase nucleus.

The nanosheet structure can be described as a combination of these two units with a glide plane: a mirror plane normal to the *b*-axis that is staggered by (1/2, 1/2) in the ac plane. On the other hand, the anatase unit cell comprises four sets of Ti1, O1, and O2 as shown in Figure 7b. These units are stacked, being related by four glide planes at $z = 1/8, 3/8, 5/8, 7/8$. One half of the anatase unit cell can be formed when one of two sets of the Ti1, O1, and O2 planes in the nanosheet is shifted with respect to each other by (1/2, 0) or (0, 1/2) in the ac plane, accompanying a change in lateral dimension (from 0.38 nm × 0.30 nm to 0.38 nm × 0.38 nm) and relative vertical location of O atoms. Here, the presence of Ti vacancies indicates that the structural change is not a genuine phase transformation, as mentioned above (eq 1). However, this may not have a significant impact on the structural modification because of the

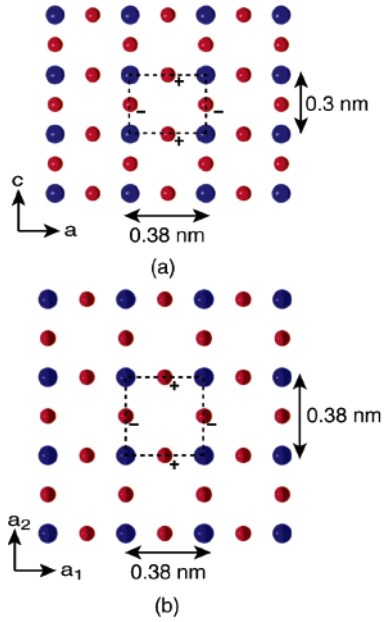

Figure 9. Atomic packing of the titanium layer and additional two oxygen layers for the titania nanosheet and anatase projected along the *b*-axis and *c*-axis, respectively. Signs, + and −, indicate the vertical displacement of O atoms with respect to the plane of Ti atoms.

limited deficiency. Consequently, rearrangement of Ti and O atoms may be attained by a relatively small energy change.

This type of structural change may be particularly favored under the experimental conditions in this study: the diffusion rate-limiting process. The nanosheets lie flat to the substrate in the films, with their a × c plane parallel to it. Consequently, the anatase nanocrystals grow with their *c*-axis perpendicular to the substrate. This speculation should be strictly valid for films with the layer number of two and less because two layers of the nanosheets roughly equal the length of the *c*-axis of anatase structure. This is actually consistent with the experimental results that these films produced highly oriented nanocrystals of anatase. The thicker films can allow crystallization in random orientation. However, the high abundance of the oriented components suggests that the crystallization mechanism using the nanosheet two-dimensional structure as a sort of template still exists in the thicker films.

The nucleation and growth of crystals have been investigated mainly for solution- and vapor-phase reactions.[1] These techniques have greatly contributed to the fabrication of a range of functional crystalline materials today. Two major examples are molecular beam epitaxy and metal organic chemical vapor deposition, with which control of crystallographic orientation of anatase films has been attained.[24] However, these methods have several restrictions for applications in principle. The substrates that can be used are limited to $SrTiO_3$ and $LaAlO_3$, because heteroepitaxial growth requires a close similarity of lattice parameters between the crystal and the substrate. During the reaction, the atmosphere should be controlled and generally kept at vacuum to supply growth units. In contrast, the present reactant system, in which the nanosheets act as both the embryo and the growth units, allows the control of coverage and orientation of anatase nanocrystals by means of the deposition number of the nanosheet layers. This novel phenomenon may be peculiar to various two-dimensional ultrathin systems and

(24) (a) Chen, S.; Mason, M. G.; Gysling, H. J.; Paz-Pujalt, G. R.; Blanton, T. N.; Castro, T.; Chen, K. M.; Fictorie, C. P.; Gladfelter, W. L.; Franciosi, A.; Cohen, P. I.; Evans, J. F. *J. Vac. Sci. Technol., A* **1993**, *11*, 2419−2429. (b) Sugimura, W.; Yamazaki, T.; Shigetani, H.; Tanaka, J.; Mitsuhashi, T. *Jpn. J. Appl. Phys.* **1997**, *36*, 7358−7359. (c) Herman, G. S.; Gao, Y. *Thin Solid Films* **2001**, *397*, 157−161. (d) Ong, C. K.; Wang, S. J. *Appl. Surf. Sci.* **2001**, *185*, 47−51.

applicable to other nanosheet systems derived from a wide variety of layered compounds.

Acknowledgment. This work was supported by CREST of the Japan Science and Technology Agency (JST) and Japan Society for the Promotion of Sciences (JSPS). The total reflection fluorescence XAFS and in-plane XRD measurements were performed with the approval of the Photon Factory Program Advisory Committee (2003G270, 2003G271, 2005G159, and 2005G239).

Supporting Information Available: Figure S1: AFM image for the as-grown monolayer film of oversized titania nanosheets. Figure S2: RHEED pattern for the monolayer sample heated at 900 °C. Figures S3 and S4: XANES spectra and in-plane XRD patterns for the five- and 10-layered films, respectively. This material is available free of charge via the Internet at http://pubs.acs.org.

JA0668116